30. Mattsson MEK, Enberg G, Ruusala A-I, Hall K, Påhlman S. Mitogenic response of human SH-SY5Y neuroblastoma cells to insulin-like growth factor I and II is dependent on the stage of differentiation. *J Cell Biol* 1986, **102**, 1949–1954.
31. Mattsson MEK, Hammerling U, Mohall E, Hall K, Påhlman S. Mitogenically uncoupled insulin and IGF-I receptors of differentiated human neuroblastoma cells are functional and mediate ligand-induced signals. *Growth Factors* 1990, **2**, 251–265.
32. Lavenius E, Parrow V, Nånberg E, Påhlman S. Basic FGF and IGF-I promote differentiation of human SH-SY5Y neuroblastoma cells in culture. *Growth Factors* 1994, **10**, 29–39.
33. Lavenius E, Gestblom C, Johansson I, Nånberg E, Påhlman S. Transfection of the ctrk gene into human neuroblastoma cells restores their ability to differentiate in response to NGF (submitted).
34. Azar CG, Scavarda NJ, Reynolds P, Brodeur GM. Multiple defects of the nerve growth factor receptor in human neuroblastoma. *Cell Growth Different* 1990, **1**, 421–428.
35. Chen J, Chattopadhyay B, Venkatakrishnan G, Ross AH. Nerve growth factor-induced differentiation of human neuroblastoma and neuroepithelioma cell lines. *Cell Growth Different* 1990, **1**, 79–85.
36. Jensen LM. Phenotypic differentiation of aphidicolin-selected human neuroblastoma cultures after long-term exposure to nerve growth factor. *Dev Biol* 1987, **120**, 56–64.
37. Jensen LM, Zhang Y, Shooter EM. Steady-state modulations associated with nerve growth factor (NGF)-induced terminal differentiation and NGF deprivation-induced apoptosis in human neuroblastoma cells. *J Biol Chem* 1992, **267**, 19325–19333.
38. LoPresti P, Poluha W, Poluha DK, Drinkwater E, Ross AH. Neuronal differentiation triggered by blocking cell proliferation. *Cell Growth Different* 1992, **3**, 627–635.
39. Anderson DJ. Molecular control of cell fate in the neural crest: the sympathoadrenal lineage. *Ann Rev Neurosci* 1993, **16**, 129–158.
40. El-Badry OM, Romanus JA, Helman LJ, Cooper MJ, Rechler MM, Israel MA. Autonomous growth of a human neuroblastoma cell line is mediated by insulin-like growth factor II. *J Clin Invest* 1989, **84**, 829–839.
41. Hedborg F, Holmgren L, Sandstedt B, Ohlsson R. The cell type-specific IGF2 expression during early human development correlates to the pattern of overgrowth and neoplasia in the Beckwith–Wiedemann syndrome. *Am J Path* 1994, **4**, 802–817.
42. Nakagawara A, Arima-Nakagawara M, Scavarda NJ, Azar CG, Cantor AB, Brodeur GM. Association between high levels of expression of the TRK gene and favorable outcome in human neuroblastoma. *N Engl J Med* 1993, **328**, 847–854.
43. Suzuki T, Bogenmann E, Shimada H, Stram D, Seeger RC. Lack of high affinity nerve growth factor receptors in aggressive neuroblastomas. *J Natl Cancer Inst* 1993, **85**, 344–345.
44. Kogner P, Barbany G, Dominicie C, *et al.* Coexpression of mRNA for trk proto-oncogene and low affinity nerve growth factor receptor in neuroblastoma with favourable prognosis. *Cancer Res* 1993, **53**, 2044–2050.
45. Borrello MG, Bongarzone I, Pierotti MA, *et al. trk* and *ret* proto-oncogene expression in human neuroblastoma specimens: high frequency of *trk* expression in non-advanced stages. *Int J Cancer* 1993, **54**, 540–545.
46. Nakagawara A, Azar CG, Scavarda NJ, Brodeur GM. Expression and function of TRKB and BDNF in human neuroblastoma. *Molec Cell Biol* 1994, **14**, 759–767.
47. Gaetano C, Matsumoto K, Thiele CJ. *In vitro* activation of distinct molecular and cellular phenotypes after induction of differentiation in a human neuroblastoma cell line. *Cancer Res* 1992, **52**, 4402–4407.
48. Ambros IM, Zellner A, Stock C, Amann G, Gadner H, Ambros PF. Proof of the reactive nature of the Schwann cell in neuroblastoma and its clinical implications. *Adv Neuroblastoma Res* 1994, **4**, 331–337.
49. Coupland R. The development and fate of catecholamine secreting endocrine cells. In Parves H, Parves S, eds. Biogenic *Amines in Development*. Amsterdam, Elsevier/North Holland, 1980, 3–28.

Pergamon

European Journal of Cancer Vol. 31A, No. 4, pp. 458–463, 1995

0959-8049/95 $9.50+0.00

0959-8049(95)00006-2

Proliferation and Apoptosis in Neuroblastoma: Subdividing the Mitosis-karyorrhexis Index

C. Gestblom, J.C. Hoehner and S. Påhlman

The Shimada classification is a frequently used, histopathological classification system for neuroblastoma tumours. Tumours are classified as prognostically favourable or unfavourable based upon stroma content, degree of neuroblastic maturation and patient age at diagnosis. The mitosis-karyorrhexis index is introduced in this classification system, as the cellular density sum of mitotic and karyorrhectic cells in the tumour. The biological nature of karyorrhectic cells is uncertain, but a high mitosis-karyorrhexis index in stroma-poor tumours is an indicator of poor prognosis. In this study, neuroblastoma tumours were analysed for cell proliferation, using antiproliferating cell nuclear antigen (PCNA) immunohistochemistry, and apoptosis, by morphology and *in situ* end-labelling of fragmented DNA. The karyorrhectic cells described in the Shimada classification were shown to be either proliferating or undergoing apoptosis. It is further shown that a high cellular density of proliferating cells correlates with poor prognosis, whereas a high density of apoptosis, in contrast, indicates favourable outcome.

Key words: mitosis-karyorrhexis index, programmed cell death, apoptosis, neuroblastoma
Eur J Cancer, Vol. 31A, No. 4, pp. 458–463, 1995

INTRODUCTION

THE BIOLOGICAL heterogeneity of neuroblastoma (NB) often causes difficulties in prognostic determination. A number of different criteria have been shown to be of prognostic importance, the most important of which include tumour stage and age of the patient at diagnosis [1, 2]. Other factors such as tumour localisation, *MYCN* amplification, neuronal *CSRC* expression, deletion of chromosome 1p, and *TRKA* expression are also of prognostic value [2–9].

A number of histopathological grading systems of NB have been proposed and employed [10–13]. In 1984 a classification system based on tumour histopathology was proposed by Shimada and associates [11]. Tumours were classified as prognostically favourable or unfavourable based upon stroma content, degree of neuroblastic maturation and nuclear histology. The mitosis-karyorrhexis index (MKI) was introduced, and reflects the density of cells with atypical nuclei, that is, mitotic cells and cells with a crescent-like, punctate, or lobulated nucleus taken together. These cells are summed together due to the difficulty in discerning cells undergoing mitosis from those defined as karyorrhectic cells. In stroma-poor NB tumours, a high MKI correlates with poor prognosis [11, 14].

Apoptosis, the sequelae of programmed cell death, can be morphologically identified as a nuclear cellular death. It is referred to as a form of cellular suicide, an active process which involves condensation and fragmentation of DNA [15–17]. Apoptotic cells can be identified both by nuclear morphology and by techniques which detect fragmented DNA [18]. Programmed cell death is not only an important event during normal embryonic development and maintenance of adult tissues, to eliminate cells that are no longer required, but it is also of importance in tumour growth [19]. Recent reports indicate that when oncogene transfected cell lines are implanted into nude mice, the overall growth rate of the resulting tumours is partly dependent upon the extent of apoptosis [19]. High levels of apoptosis correlate with slower tumour growth.

When NB tumours were analysed with regard to apoptosis, a positive correlation between high levels of apoptosis and good prognosis could be established [20]. Based on the nuclear similarities of apoptotic cells and karyorrhectic cells of the MKI, these results seemed rather contradictory to the results of Shimada and colleagues, where a high MKI correlates with poor prognosis [11]. We therefore analysed the cells of the MKI further, investigating whether the MKI could be subdivided into two groups, mitotic cells and apoptotic cells. We hypothesised that a high density of mitotic cells in neuroblastoma would then correlate with poor prognosis, according to the MKI of Shimada, whereas a high density of apoptotic cells would rather portend good prognosis. This investigation utilises a selection of clinical NB tumour specimens. The MKI was determined according to Shimada and associates and proliferation analysed using an antibody specific for the proliferating cell nuclear antigen (PCNA). The density of apoptotic cells was measured by nuclear morphology and *in situ* DNA fragmentation end-labelling.

MATERIALS AND METHODS

Pathological materials

Pertinent clinical features and materials were obtained from 39 patients registered and treated for NB [31], ganglioneuroblastoma [5], or ganglioneuroma [3] in Sweden over the past 7 years. Pathological materials from biopsy or resection of primary or metastatic tumour were evaluated, and the diagnosis was confirmed at one of four referral hospitals in Göteborg, Lund, Stockholm, or Uppsala, Sweden. Tumour stage was determined clinically or at the time of surgical biopsy or resection according to the criteria of Evans and colleagues [1]. Patients' characteristics were obtained from the treating clinicians. Of 10 patients diagnosed with Stage I or Stage II disease, all remain alive and free of disease at median follow-up of 31 months. Of the 12 patients with Stage IV disease, 7 have died (58%), 2 patients remain alive with active disease, and 3 patients remain free of disease at a median follow-up of 29 months. Patients were at varying stages of treatment at the time of tissue acquisition. The majority of patients with Stage III and Stage IV disease (60%) received cytotoxic therapy prior to the time of tumour biopsy or resection whereas those with Stage I, II, and IVS had not (0%).

Tissue preparation

Tissue samples were fixed in 4% buffered formaldehyde and embedded in paraffin. Sections of 4–5 μm were secured to slides pretreated with silane and acetone. Deparaffinisation was performed by baking slides overnight at 37°C, and transfer of slides through xylene and progressive dilutions of ethanol to deionised distilled water (DDW).

Immunohistochemistry of tissue sections

Sections were subjected to microwave treatment in 10 mM sodium citrate buffer, pH 7.3, for 5 min at 750 watts, and 10 min at 450 watts. Sections were then blocked with 0.1% bovine serum albumin (BSA) in Tris–HCl buffered saline (TBS) for 20 min. Mouse monoclonal PCNA antibody (Boehringer Mannheim, Germany), diluted 1:50 was added to sections and incubated for 60 min at room temperature (RT). Slides were rinsed 3 times with TBS and incubated for 30 min at RT with AP-conjugated antimouse antibody (Sigma, St Louis, U.S.A.) at 1:40 dilution. Sections were again washed 3 times with TBS, and developed using Napthol-AS-MX-phosphate as a chromogen according to manufacturers instructions (Dakopatts, Copenhagen, Denmark). Slides were then rinsed in tap water for 10 min and sections counterstained with haematoxylin for 30 s. Cover slips were applied in aqueous medium. Negative controls were obtained by exclusion of primary and/or secondary antibody or by incubation with non-immune bovine serum albumin at equivalent concentrations. The antiPCNA antibody specifically recognises a proliferating cell nuclear antigen found on cyclin and the auxiliary protein of DNA polymerase delta. This antigen is expressed during all phases of the cell cycle excluding G_0 [20].

DNA nick end-labelling of tissue sections

A procedure to specifically end-label DNA cleavage sites in tissue sections *in situ* (TUNEL) was employed as previously described with minor modifications [18, 20]. Paraffin embedded sections were deparaffinised as described above and incubated in a moist chamber for 15 min with 20 μg/ml proteinase K (Sigma, St Louis, U.S.A.), and thereafter washed 3 times with DDW. Hydrogen peroxide at 2% was added for 5 min to inactivate endogenous peroxidase, and the sections were again washed 3 times in DDW. Each section was then incubated at 37°C for 60 min with terminal deoxynucleotidyl transferase (10 e.u./50 μl) and biotinylated deoxyuridine (dUTP) (0.5 nmol/50 μl) (both Boehringer Mannheim, Mannheim, Germany) in transferase buffer (30 mM Tris HCl buffer of pH 7.2, 140 mM

Correspondence to S. Påhlman.
All authors are at the Department of Pathology, Uppsala University Hospital, S-751 85 Uppsala, Sweden.

sodium cacodylate, and 1 mM cobalt chloride). The reaction was terminated by immersion in 300 mM NaCl, 30 mM sodium citrate buffer for 15 min. Sections were washed with DDW 3 times, blocked for 10 min with 2% BSA at room temperature, and washed again with DDW 3 times. Sections were immersed in phosphate buffered saline (PBS) for 5 min and then incubated with ABC complex (1:100 avidin, 1:100 biotinylated horseradish peroxidase, in 0.1% BSA) (Dakopatts) for 30 min according to the manufacturers instructions. Sections were washed with DDW 3 times, immersed in PBS for 5 min, developed with 3-amino-9-ethylcarbazole as chromogen for 10 min at RT, washed for 10 min in DDW, and cover slips were applied in aqueous medium.

Combined PCNA immunohistochemistry and TUNEL analysis

Sections were double processed by antiPCNA antibody immunohistochemistry and thereafter by TUNEL as described above, with minor modifications. Immunohistochemistry was performed first, using BCIP/NBT (Sigma) as chromagen. TUNEL processing followed, with exclusion of proteinase K treatment. In these double-stained sections, counterstaining was not necessary.

Quantitation of MKI, proliferation and apoptosis

All tumours were processed and analysed blindly without knowledge of tumour stage or patient outcome. The average number of cells in a high power field (400x magnification) was determined on routine haematoxylin and eosin sections. Tumour regions representative of each specimen were chosen for analysis, and stroma-rich capsules or necrotic areas were avoided. Only tumour cells were included in the analysis, excluding cells such as lymphocytes, stroma cells, and red blood cells. Several different high power fields were counted for immunoreactivity with PCNA antibody on each tumour, until at least 5000 cells in total per tumour were analysed. The total number of PCNA positive cells was then determined and the density percentage per 5000 cells calculated. The same procedure was repeated on consecutive sections with regard to TUNEL positivity. Care was taken such that the same representative tumour areas were analysed for both apoptosis and PCNA positivity. Statistical analysis of the results was performed using the Student *t*-test. Statistical significance was achieved if the *P* value was less than 0.05.

The MKI was determined in accordance with Shimada and associates [11]. Tumour cells with typical spindle-shaped nuclei of mitosis were included in the index, as were cells with punctate, lobulated, or crescent-like nuclei. The total number of mitotic and karyorrhectic cells per 5000 cells were counted in randomly selected representative fields. The MKI was then placed into one of the three Shimada categories: (1) low, less than 100 mitotic-karyorrhectic cells per 5000 tumour cells; (2) intermediate, 100–200 mitotic-karyorrhectic cells per 5000 tumour cells; or (3) high, more than 200 mitotic-karyorrhectic cells per 5000 tumour cells.

RESULTS

Histologic determination of apoptosis and karyorrhexis

A procedure which enzymatically visualises fragmented DNA *in situ* by synthesis of a biotinylated dUTP polymer, referred to as TUNEL, provides a means of identifying cells undergoing programmed cell death, or apoptosis. TUNEL staining is nuclear specific, with positively stained neuroblasts identified in all tumours analysed. The density of apoptotic cells, and the distribution of these cells within a tumour, varied from specimen to specimen (Table 1, Figure 1). In high stage tumours, apoptotic cells were visualised in a randomly scattered pattern, whereas in lower stage tumours apoptotic cells were more commonly found in groups. TUNEL positive cells displayed a nuclear morphological appearance typical of apoptosis, with condensed and fragmented nuclei, often with the formation of typical apoptotic bodies (Figure 2). The majority of the TUNEL positive neuroblasts would also be classified as karyorrhectic based upon their nuclear morphology (Figure 2B).

Tumour specimens were subdivided into two groups based upon ultimate patient survival. Statistically significant increased

Table 1. PCNA, TUNEL and patient characteristics of tumours studied

Status	Stage	Age dx	(% PCNA)	% TUNEL	MKI
NED	1	1 y	5.1	0.35	high
NED	1	2 mo	11.4	6.5	high
NED	1	1 mo	7.0	0.4	int
NED	1	birth	8.7	2.3	low
NED	1	2 mo	1.6	0.4	int
NED	1	birth	11.4	4.7	high
NED	2	3 mo	16	1.0	int
NED	2	18 mo	11	1.2	high
NED	2	6 mo	7.5	0.5	low
NED	2	8.5 y	4.0	0.2	high
NED	3	3.5 y	36	1.1	int
NED	3	13 mo	13	1.6	int
NED	3	7 mo	6.5	1.0	int
NED	3	12 mo	1.0	1.0	low
NED	4	32 mo	11	0.7	low
NED	4	10 mo	25	1.4	int
NED	4	3.5 y	13.6	6.9	high
DOD	3	5 y	0.6	0.7	low
DOD	3	birth	17	1.3	high
DOD	4	7 y	3.7	0	low
DOD	4	3 y	2.2	0.1	high
DOD	4	10 mo	13	0.4	high
DOD	4	6 y	70	0	high
DOD	4	4.5 y	88	0.2	high
DOD	4	6.5 y	12	0.25	high
DOD	4	3 mo	20	0	high
act dz	4	4.5 y	69	1.5	high
act dz	4	10 mo	20	0.3	high
NED	4S	birth	28	0	int
DOD	4S	birth	33	0	int
act dz	4S	5 mo	18	0	high
NED	GN	5 y	8.4	0.1	
NED	GN	4.5 y	24.6	0	
NED	GN	29 mo	2.0	1.0	
NED	Gnb	1 mo	8.8	1.0	
NED	Gnb	3.5 y	18	0	
NED	Gnb	3.5 y	29	0.1	
DOD	Gnb	10 mo	9.0	0.8	
DOD	Gnb	6.5 y	77	0	

Tumours were grouped into survivors (NED; no evidence of disease; act dz, active disease) and non-survivors (DOD; dead of disease). Neuroblastoma tumours were staged according to Evans and associates [1]. % PCNA and % TUNEL represent cellular density per cent positivity of each tumour for either PCNA immunostaining or TUNEL. Age at diagnosis (AGE dx) and mitosis-karyorrhexis index (MKI) are also listed. The MKI is categorised as high, intermediate (int) and low. GN, ganglioneuroma; Gnb, ganglioneuroblastoma.

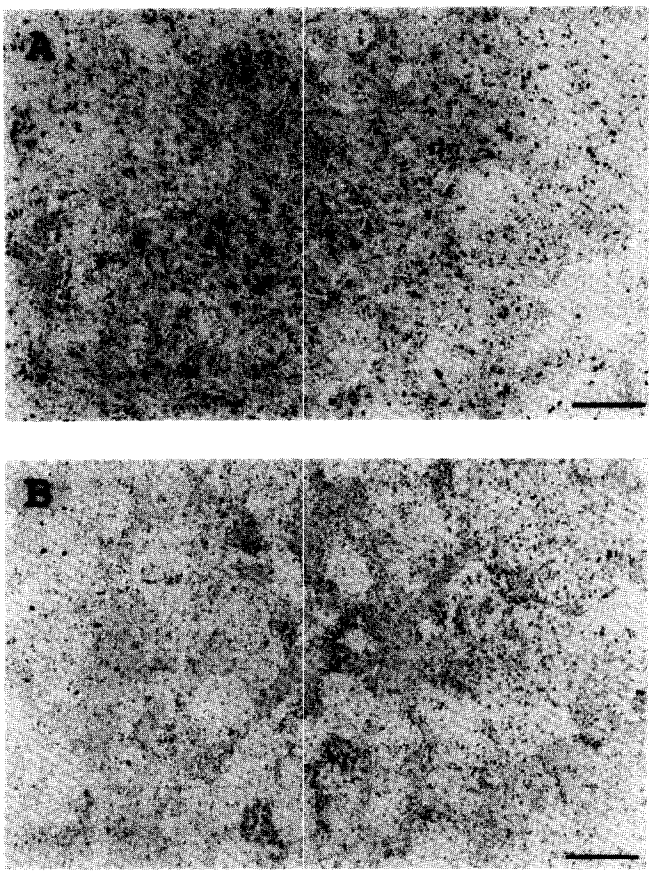

Figure 1. (A) Low power photomicrograph of proliferating cells in a stage 1 neuroblastoma tumour detected by antiproliferating cell nuclear antigen (PCNA) immunohistochemistry. Positive cells indicated by dark signals. (B) Cells undergoing apoptosis in the same tumour, visualised by TUNEL. Scale bars: 80 μm.

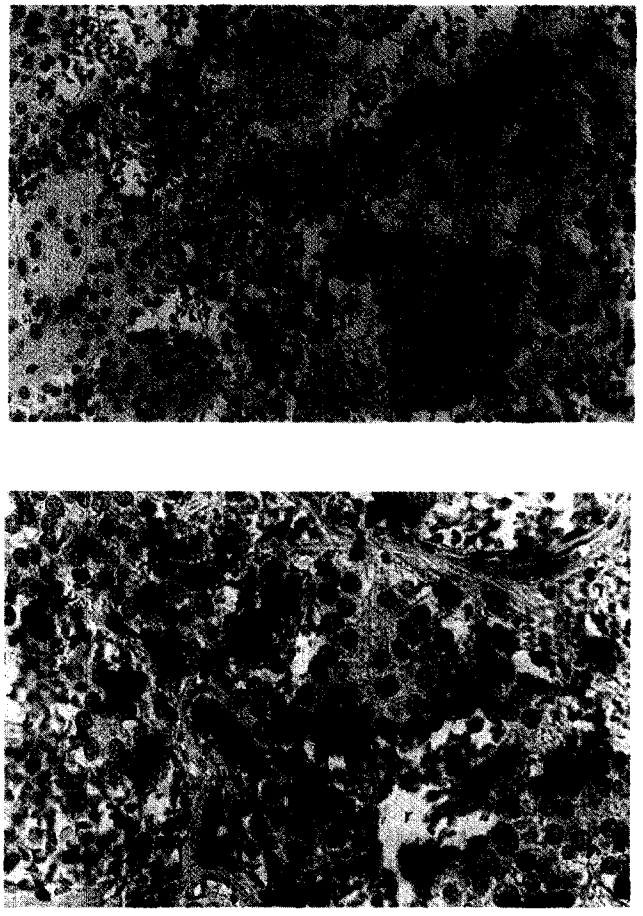

Figure 2. (A) Double-stained neuroblastoma tumour, showing proliferating and apoptotic cells simultaneously. Proliferating cells are dark blue, and TUNEL positive cells are deep red. Note that the number of proliferating cells far exceed the apoptotic density. (200x magnification) (B) High power field (400x) of the same tumour as in (A), in an area rich in apoptosis. Note three cells with similar morphology (arrowheads) differing in staining; one is TUNEL positive (red), another PCNA positive (blue), and the third negative to both. Note that a typically appearing karyorrhectic cell is TUNEL positive (curved arrow).

apoptotic cellular density was evident in tumours of surviving patients (1.74 ± 0.49%) versus those who died (0.36 ± 0.50%), (P = 0.015).

Several ganglioneuromas and ganglioneuroblastomas were also analysed with regard to apoptosis and proliferation. The results are shown in Table 1. Surprisingly high proliferation levels and low apoptotic levels were evident in two of the ganglioneuromas, as well as in the ganglioneuroblastomas. No statistical comparisons were performed on these tumours.

PCNA immunoreactivity in neuroblastoma tumours

Proliferating cells were detected with the antiPCNA antibody, which is specific for a nuclear antigen expressed during all stages of the cell cycle excluding G_0 [21]. The nuclear morphology of the majority of PCNA positive cells was unremarkable, and thus would not have been included in the MKI (Figure 2). There were, however, many positive cells that were obviously mitotic. Some of the PCNA positive cells displayed a nuclear appearance typical of karyorrhectic cells, rather than of mitotic cells, again confirming the difficulty in distinguishing mitosis and karyorrhexis.

The density of proliferating cells varied between tumours, and within tumours, and was generally considerably higher than the density of apoptotic cells (Table 1, Figure 1). Even in specimens with high TUNEL positivity, PCNA staining density was far greater than TUNEL (Figure 1). When the patients were divided into survivors and those who had died, a weak correlation between high proliferation density (PCNA immunoreactivity) and poor prognosis was evident (P = 0.07).

When the density of proliferating cells was analysed within the survivor group, there appeared to be a connection between high PCNA density and high TUNEL positivity, i.e. tumours with high proliferation also had high TUNEL. This was not true for those that died nor for the 4S patients, where apoptosis levels were low independent of proliferation. The proliferation/apoptosis pattern of the 4S patients differs from other tumours. They all have extremely high proliferation densities and virtually no TUNEL positivity. NB tumours of all stages except 4S are plotted with regard to PCNA and TUNEL positivity (Figure 3). Tumours are here categorised based upon patient outcome, and a trend towards high TUNEL density and proliferation density in surviving patients is evident. The corollary is also true.

A statistical comparison of the sum of mitotic and apoptotic densities between survivors and those that died was also performed, but no statistically significant differences were evident (P = 0.1).

MKI

When proliferation, as measured by PCNA staining, and apoptosis, detected by TUNEL positivity, are summed together,

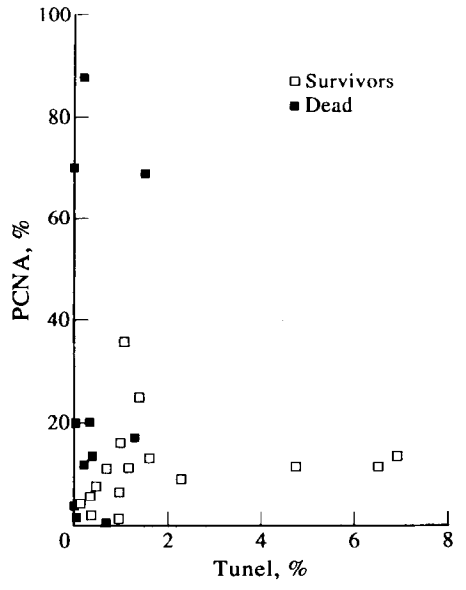

Figure 3. Neuroblastoma tumours of all stages except 4S are plotted with regard to antiPCNA immunoreactivity and TUNEL density. Survivors (open boxes) tend to have higher TUNEL positivity than do those who died (solid boxes).

the resulting cellular density typically exceeds the determined MKI. Morphologically, the nuclei of PCNA positive cells are very often normal in appearance. The molecular changes of mitosis within these cells are not morphologically detectable, thereby explaining why they are not included in the MKI. TUNEL positive cells more often show a karyorrhectic appearance, but this is not always the case. Analysis of sections stained with both PCNA and TUNEL simultaneously revealed that all identifiable karyorrhectic cells were found to be either PCNA or TUNEL positive (Figure 2B).

DISCUSSION

Based upon the difficulty in distinguishing purely mitotic cells from other karyorrhectic cells, they are counted together to give the MKI. In NB it is known from the work of Shimada, and others, that a high MKI indicates a poor prognosis [11, 14]. In this work, the possibility of subdividing the cells comprising the MKI into putative subgroups was investigated, as well as the prognostic consequences of such subdivisions. Based on previous results, where a positive correlation between high levels of apoptosis and good prognosis was seen [20], it seemed possible that division of the MKI into two different parameters, mitosis and apoptosis, might add further prognostic information for NB patients.

Analysis of NB tumours using the TUNEL technique confirmed that a number of the cells described as karyorrhectic were actually apoptotic. This was expected, but it was interesting that many cells with fragmented DNA would not be defined as karyorrhectic based on morphology alone. When we analysed the apoptotic cellular density in tumours of surviving NB patients, and compared it with tumours of those who had died, previous results could be confirmed [20]. High apoptosis levels in a tumour correlated with improved patient survival. Interestingly, this was independent of the number of proliferating cells. Statistical comparisons of our tumour material indicated that apoptotic density was of greater prognostic importance than PCNA positivity. High proliferation alone correlated with unfavourable patient outcome, but not with statistical significance in this study.

When proliferation and apoptosis were added together in each tumour, a density exceeding the determined MKI was often achieved. Since MKI is solely a morphological index, it is not surprising that the use of molecular markers expands the cells included in the index. However, it is interesting that when double-stained sections were analysed, we found no karyorrhectic cells that were negative to both PCNA and TUNEL staining. Karyorrhectic cells were found to be either mitotic cells, with a somewhat unusual nuclear morphology, or cells undergoing apoptosis.

We have shown that the MKI is the morphological sum of proliferating and apoptotic cells in NB tumours. The MKI has been previously reported as a valid indicator of tumour prognosis for NB patients, but it is interesting that the two cellular events included in the MKI actually indicate two different biological processes. Since the density of proliferating cells so very often outnumbers apoptosis, the resultant sum relies most heavily on proliferation, and thus a high MKI correlates with poor prognosis. Quantitation of apoptotic and proliferation densities in solid tumours, such as NB, may be of use in tumour grading, predicting prognosis, determining tumour aggressiveness, and evaluating treatment response.

1. Evans AE, D'Angio GJ, Randolph JA. A proposed staging for children with neuroblastoma. Childrens cancer study group A. *Cancer* 1971, **27**, 374–378.
2. Coldman AJ, Fryer CJH, Elwood JM, Sonley MJ. Neuroblastoma: influence of age at diagnosis, stage, tumor site and sex on prognosis. *Cancer* 1980, **46**, 1896–1901.
3. Hedborg F, Bjelfman C, Sparén P, Sandstedt B, Påhlman S. Biochemical evidence for mature phenotypes in morphologically poorly differentiated neuroblastomas with favourable outcome. *Eur J Cancer* 1995, **31A**, 435–443.
4. Brodeur GM, Fong CT, Morita M, Griffith R, Hayes FD, Seeger RC. Molecular analysis and clinical significance of N-*myc* amplification and chromosome 1p monosomy in human neuroblastomas. *Prog Clin Biol Res* 1988, **271**, 3–15.
5. Schwab M, Varmus HE, Bishop JM, *et al.* Chromosome localization in normal human cells and neuroblastomas of a gene related to c-*myc*. *Nature* 1984, **308**, 288–291.
6. Bjelfman C, Hedborg F, Johansson I, Nordenskjöld M, Påhlman S. Expression of the neuronal form of $pp60^{c\text{-}src}$ in neuroblastoma in relation to clinical stage and prognosis. *Cancer Res* 1990, **50**, 6908–6914.
7. Heim S, Mitelman F. *Cancer Cytogenetics*, Alan R. Liss, 1987. New York.
8. Nakagawara A, Asima-Nakagawara M, Scavarda NJ, Azar CG, Cantor AB, Brodeur GM. Association between high levels of expression of the trk gene and favourable outcome in human neuroblastoma. *New Engl J Med* 1993, **328**, 847–854.
9. Seeger RC, Brodeur GM, Sather H, *et al.* Association of multiple copies of the N-*myc* oncogene with rapid progression of neuroblastomas. *New Engl J Med* 1985, **313**, 1111–1116.
10. Beckwith JB, Martin RF. Observations on the histologic theory of neuroblastomas. *J Pediatr Surg* 1968, **3**, 106–110.
11. Shimada H, Chatten J, Newton WA, *et al.* Histopathologic prognostic factors in neuroblastoma tumors: definition of subtypes of ganglioneuroblastoma and an age linked classification of neuroblastoma. *J Natl Cancer Inst* 1984, **73**, 405–416.
12. Joshi VV, Cantor AB, Altshuler G, *et al.* Recommendations for modifications of terminology of neuroblastic tumors and prognostic significance of Shimada classification. *Cancer* 1992, **69**, 2183–2196.
13. Joshi VV, Cantor AB, Altshuler G, *et al.* Age-linked prognostic categorization based on a new histologic grading system of neuroblastomas. *Cancer* 1992, **69**, 2197–2209.
14. Joshi VV, Chatten J, Sather HN, Shimada H. Evaluation of the Shimada classification in advanced neuroblastoma with a special

reference to the mitosis-karyorrhexis index: a report from the childrens cancer study group. *Mod Pathol* 1991, **4**, 139–147.
15. Arends MJ, Morris RG, Wyllie AH. Apoptosis: the role of the endonuclease. *Am J Pathol* 1990, **136**, 593–608.
16. Wyllie AH, Kerr JFR, Currie AR. Cell death: the significance of apoptosis. *Int Rev Cytol* 1980, **68**, 251–306.
17. Wyllie AH. Glucocorticoid induced thymocyte apoptosis is associated with endonuclease activation. *Nature* 1980, **284**, 555–556.
18. Gavrieli Y, Sherman Y, Ben-Sasson SA. Identification of programmed cell death *in situ* via specific labeling of DNA fragmentation. *J Cell Biol* 1992, **119**, 493–501.
19. Arends MJ, Angus HM, Wyllie AH. Apoptosis is inversely related to necrosis and determines net growth in tumors bearing constitutively expressed *myc, ras* and HPV oncogenes. *Am J Pathol* 1994, **144**, 1045–1057.
20. Hoehner JC, Hedborg F, Jernberg Wiklund H, Olsen L, Påhlman S. Cellular death in neuroblastoma: *in situ* correlation of apoptosis and *bcl-2* expression (unpublished).
21. Kurki P, Ogata K, Tan EM. Monoclonal antibodies to proliferating cell nuclear antigen (PCNA)/cyclin as probes for proliferating cells by immunofluorescence microscopy and flow cytometry. *J Immun Methods* 1988, **109**, 49–59.

Acknowledgements—Supported by the Children Cancer Foundation of Sweden, Swedish Cancer Society, HKH Kronprinsessan Lovisas förening för barnasjukvård, American-Scandinavian Foundation, Hans von Krantzows and Ollie och Elof Ericssons Stiftelser.

Pergamon

European Journal of Cancer Vol. 31A, No. 4, pp. 463–466, 1995

0959–8049/95 $9.50+0.00

0959-8049(95)00059-3

Cell Death by Oxidative Stress and Ascorbic Acid Regeneration in Human Neuroectodermal Cell Lines

V. De Laurenzi, G. Melino, I. Savini, M. Annicchiarico-Petruzzelli, A. Finazzi-Agrò and L. Avigliano

In this paper, we show that human neuroectodermal cells exposed to 1–5 mM hydrogen peroxide or 10 nM–1 mM ascorbate die by programmed cell death induced by oxidative stress. The cell death by peroxide occurs within 4 h and involves approximately 80% of B-mel melanoma cells, while ascorbate causes cell death of approximately 86% of B-mel cells within 24 h. SK-N-BE(2) neuroblastoma cells are more resistant, 32% and 43% cell death for peroxide and ascorbate, respectively. In all cases, cell death causes hypodiploic DNA staining, evaluated by flow cytometry. Both cell lines can efficiently metabolise ascorbate due to significant levels of NADH-dependent semidehydroascorbate reductase and glutathione-dependent dehydroascorbate reductase. The cell death observed suggests a pro-oxidant, rather than anti-oxidant, role for ascorbic acid at physiological concentrations under these experimental conditions.

Key words: apoptosis, ascorbic acid, cell death, hydrogen peroxide, melanoma, neuroblastoma
Eur J Cancer, Vol. 31A, No. 4, pp. 463–466, 1995

INTRODUCTION

CELL DEATH by apoptosis is a gene-regulated programme of cell self-deletion acting under physiological conditions in multicellular organisms, characterised by specific nuclear (chromatin condensation, DNA fragmentation) and cytoplasmic (integrity of the cell membrane with formation of stable protein cross-links catalysed by tissue-transglutaminase, EC 2.3.2.13, thus conferring resistance to breakage and chemical attack to the apoptotic body) events [1, 2]. The negative control of apoptosis is maintained by ced-9 in *C. elegans* [3], by bcl-2 [4, 5] and possibly other gene products [6–8] in vertebrates. Recently, additional members of the *BCL-2* gene family have been isolated, *BCL-X* and *BAX*, that may act synergistically or antagonistically with *BCL-2* [9, 10]. bcl-2 seems to function as a cell death suppressor protein by decreasing the generation of reactive oxygen species [11, 12]. The kinetics of cell death induced by hydrogen peroxide seem to suggest that it acts on downstream effector elements with respect to *BCL-2*.

Vitamin C (ascorbic acid) is involved in many metabolic processes where it acts as an electron donor. The reduced form, ascorbate (AA), is oxidised either by single electron transfer with

Correspondence to G. Melino in via Tor Vergata 135, 00133 Rome, Italy.
V. De Laurenzi, G. Melino and M. Annicchiarico-Petruzzelli are at the Biochemistry Laboratory IDI-IRCCS, Department of Experimental Medicine, University Tor Vergata, Rome, and the Biology Department, University of L'Aquila, L'Aquila; and I. Savini, A. Finazzi-Agrò and L. Avigliano are at the Department of Experimental Medicine and Biochemical Sciences, University Tor Vergata, Rome, Italy.

EJC 31:4-D